This is a repository copy of *Ultrafast High-Resolution Solar Cell Cracks Detection Process*.

White Rose Research Online URL for this paper:
https://eprints.whiterose.ac.uk/177723/

Version: Accepted Version

Article:
Dhimish, Mahmoud and Mather, Peter (2020) Ultrafast High-Resolution Solar Cell Cracks Detection Process. Industrial Informatics, IEEE Transactions on. pp. 4769-4777. ISSN 1551-3203

https://doi.org/10.1109/TII.2019.2946210

Reuse
Items deposited in White Rose Research Online are protected by copyright, with all rights reserved unless indicated otherwise. They may be downloaded and/or printed for private study, or other acts as permitted by national copyright laws. The publisher or other rights holders may allow further reproduction and re-use of the full text version. This is indicated by the licence information on the White Rose Research Online record for the item.

Takedown
If you consider content in White Rose Research Online to be in breach of UK law, please notify us by emailing eprints@whiterose.ac.uk including the URL of the record and the reason for the withdrawal request.

eprints@whiterose.ac.uk
https://eprints.whiterose.ac.uk/

Ultra-Fast High-Resolution Solar Cell Cracks Detection Process

Abstract— **This paper presents the advancement of an ultra-fast high-resolution cracks detection in solar cells manufacturing system. The aim of the developed process is to (i) improve the quality of the calibrated image taken by a low-cost conventional electroluminescent (EL) imaging setup, (ii) proposing a novel methodology to enhance the speed of the detection of the solar cell cracks, and finally (iii) develop a proper procedure to decide whether to accept or reject the solar cell due to the existence of the cracks. The proposed detection process has been validated on various cracked/free-crack solar cell samples, evidently it was found that the cracks type, size and orientation are more visible using the proposes method, while the speed of calibrating the EL images are in the range of 0.1s to 0.3s, excluding the EL imaging time.**

Index Terms— Photovoltaic; Solar cells; Micro cracks; Electroluminescence.

I. INTRODUCTION

Micro cracks are a sincere problem in Photovoltaic (PV) solar cells. So as to examine the cracks in solar cells, multiple methods have been proposed. One of the first methods is the Resonance ultrasonic vibrations (RUV) which is developed by [1] and [2]. This method uses ultrasonic vibrations of a tenable frequency of an optical sensor. The solar cell wafer is controlled by a piezoelectric transducer in a frequency ranging from 20 to 90 kHz. The transducer contains a vital hole allowing a vacuum pairing among the wafer and the transducer using a 50 kPa negative pressure to the rear side of the solar wafer. This method is sensitive to the actual micro crack location, besides it can be used to accept or reject solar wafers though a manufacturing progression. Though, it does not classify precisely the cracks orientation, size or the exact position of the cracks in the inspected solar wafers.

Another method called Photoluminescence (PL) was proposed to solve this problem, as it could be used to inspect solar cells cracks in silicon wafers and medium to large scale cells areas [3]. PL method can be practical not only at the end of the solar cell's manufacture process, but also it could be situated during the procedure of production for solar cells [4]. Y. Zhu *et al.* [5] developed a novel PL system that allows inhomogeneous solar illumination in order to determine various parameters of solar cells. Results shows that the usage of inhomogeneous illumination meaningfully ranges the photoluminescence imaging applications for the classification of silicon wafers and solar cells.

In recent times, the PL images are attained using the solar radiation as the singular lighting source by extrication the fragile luminescence signals from the abundant sunlight illumination. This has been formed using an appropriate filtering system located amongst the normal operating threshold and open circuit conditions of a typical solar cell manufacturing system [6].

On the other hand, Electroluminescence (EL) method is another way to inspect solar cells micro cracks. By connection the solar cell sample into a forward bias mode, a current would be generated, hence, the electrons of the solar cell are excited into the conduction band whereby the image of the EL can be observed. This technique is commonly used in industry practices, since it can be used not only with small scale solar cell dimensions, and in addition to, it can be used with full scale PV panels [7] and [8]. The EL method requires the solar cells to be in the forward biased in order to radiate infrared contamination. The EL radiations ranges from 950 to 1250 nm with the peak-power occurs roughly around 1150 nm. Emission strength is reliant on the density of defects in the solar cell sample, with fewer defects/cracks resulting in an extra emitted photons [9]. The EL method should be placed in a dark room, as the image of the cells is being taken by cooled CCD camera, we have already published the structure and construction of the EL setup in [10].

So that to comprehend the impact of solar cells micro cracks, J. Käsewieter *et al.* [11] observed the influence of solar cells cracks on the performance of multiple PV cells using EL detection method. The outcome of this article proves that micro cracks at least reduces the output power of a PV cells by 2.5%. The distribution and orientation of crystalline solar cells micro cracks was primarily obtained by Z. Liu *et al.* [12]. Solar cells micro cracks were categorized into six different types, illustrated as follows: dendritic, several, +45°, -45°, parallel and perpendicular to busbars. The examination have been carried out using 27 different PV modules using EL imaging method, where the extreme micro cracks found in the PV modules is parallel to busbars with 50% relative occurrence. Moreover, the current-voltage curve analysis based on gallium arsenide (GaAs) solar cells have been inspected by S. Oh *et al.* [13]. It was evident that the yield voltage of the solar cells increase while decreasing the micro crack size.

So far, there is lack of approaches that have been able to detect the thermography images of defected solar cells using a noncontact methods. Recently, Y. He *et al.* [14] proposed a novel solution to this problem using a noncontact electromagnetic induction excited infrared thermography technique that is able to adequately inspect PV cracks, scratches, hot-spots and surface impurities.

Furthermore, there are several attempts to outline the main methods used to enhance the detection of micro cracks in solar cells. For instance, M. Abdelhamid *et al.* [15] has reviewed most current methods that are used to detect micro cracks, where it was found that 22.4% of current research is currently using EL imaging systems. Likewise, a nondestructive inspection evaluation of more than 120 recent studies have used either PL or EL method in order to investigate the impact of micro cracks affecting PV modules, B. Du *et al.* [16].

This paper presents a micro cracks solar cell detection setup using the conventional EL imaging procedure. The EL process has been previously discussed in former articles such as [7] and [17]; for ease of visualizing, a typical EL imaging setup is shown in Fig. 1(a). The main impact of the present work in this article is to improve the quality of the output images attained using a low-cost EL setup. To do so, we have developed a novel method using ORing technique that is able to analyse the examined solar cell EL image and compare it with an EL reference (healthy) solar cell image. The ORing method confirms that the micro cracks are more visible compared with conventional EL images. Furthermore, an accept/reject criterion has been proposed to either accept or reject the solar cell wafer due to the presence of micro cracks. In addition, the proposed solar cell inspection system could be used to inspect cracks in either Polycrystalline silicon (Poly-Si) or Monocrystalline silicon (Mono-Si) solar cells.

This remaining sections of this article is organized as follows: section II describes the solar cell inspection system, while section III shows the main features of the proposed technique. Section IV presents the accept/reject criterion. Section V describes the inspected speed of the proposed system, while last section, section VI comprehensively analyses the differences between the proposed technique is this article with multiple techniques available in the literature.

II. Solar Cell Inspection System

The developed solar cell inspection system consists of multi-layer procedure, as shown in Fig. 1(b). The initial solar cell is passed into a solar cell manufacturing assembling line, at this stage the solar cell is fully manufactured, hence ready to send though an inspection system.

The solar cell MES setup includes an EL imaging unit which operates in a black-box (no light or emission is permitted) in order to capture the EL image of the factory-made solar cell sample. The EL setup consists of a digital camera which is equipped with a typical 18–55 mm lens. In our setup a SensoCam [25] was used, but in principle any digital camera with similar grade CCD or CMOS sensor and where the IR filter can be removed would serve the purpose; please see Appendix A for CCD camera specifications. A power supply is applied to the solar cell in order to capture the EL image, the biasing at the short circuit current was applied to guarantee a reasonable quality output image of the cell cracks. Since the dimensions of the solar cell is fixed at the manufacturing system, therefore, there are two external metal at the rear of the assembling line that would inject the current into the solar cell during the EL inspection process.

LabVIEW software was used to handle the developed algorithm in order to accept/reject the solar cell due to the existence of the cracks in the inspected sample.

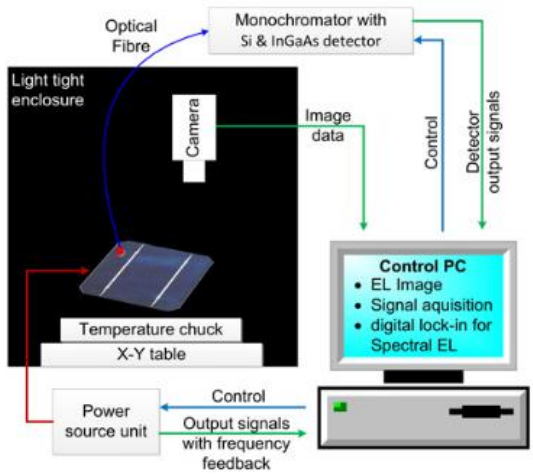

(a)

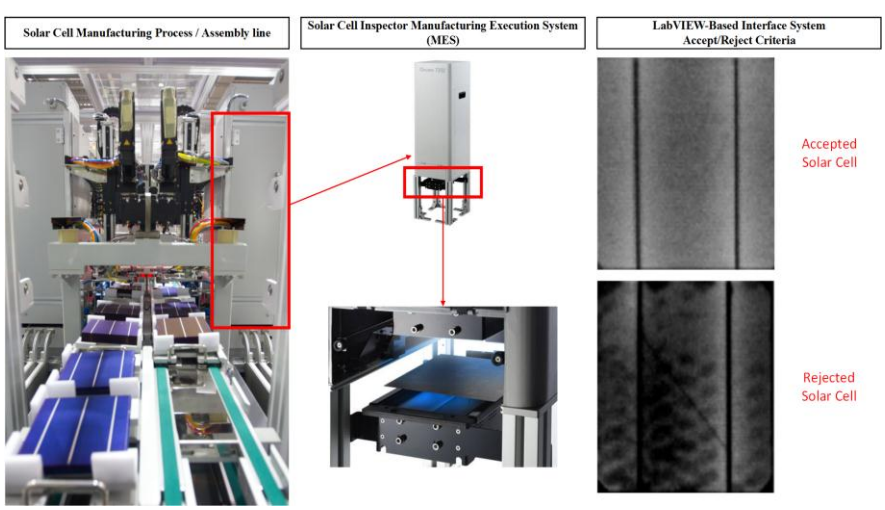

(b)

Fig. 1. (a) Typical EL imaging system [18], (b) Solar cell manufacturing and inspection system

III. Enhancing Solar Cell Micro Cracks Detection

Detecting micro cracks in solar cells faces a big challenge, particularly the cost of the detection/inspection systems such as the EL setup. While in this article we have tackled this challenge by adapting a novel algorithm into a low-cost CCD camera setup that could be used to accurately detect micro cracks in solar cell samples. While, the presence of the cracks in the output images are determined using a balk area/zones which allows us to further improve the quality and the detection of the cracks. As shown in Fig. 2, we have used an ORing method in order to function the detection of the cracks in the inspected solar cell samples. In principle, The ORing gate would compare each of the pixels in the cracked/inspected solar cell samples by a healthy solar cell image. Resulting a combination between each of the pixels, hence, if the output is equal "0", therefore, there is no crack is detected in this particular pixel, while if the output is equal to "1", meaning that the output image would be expected to have a blacked area which corresponds to the actual crack/scratch in the examined solar cell.

The procedure of the ORing method is presented in Fig. 4. The first phase is show in Fig. 4(a), where the examined solar cell output EL image is determined and compared with the healthy solar cell sample (reference sample). It is worth noting that the healthy solar cell sample is already available in the software prior to the inspection of the examined solar cell. Consequently, the ORing bit-by-bit method is applied for both images (inspected vs. reference) in order to observe the output yielded image of the cracks as shown in Fig. 4(b). By contrast with the result of the ORing method, it is evident that the healthy/reference solar cell sample bits are equal to "0"; it is only equal to "1" at the busbar levels where there is a black area covering these particular locations of the image. The output bit of the ORing method could be either "1" or "0", where "1" corresponds to an actual crack present in the examined solar cell, and "0" corresponds to non-cracked area. An example of the ORing method is shown in Fig. 4(c), the output of the OR gate is equal to "1" which corresponds to an actual crack affecting this area of the inspected solar cell. On the other hand, Fig. 4(d) shows an example of the ORing method while the output is equal to "0", resulting a non-cracked area in the yielded image.

One of the greatest limitation in the conventional EL technique that the black areas are usually present in the image. This black zone not necessary matches a crack in the solar cell/wafer, however added noise is normally calibrated using the EL setup, whereas the micro cracks orientation, size, or type are hardly to classify. Subsequently, our proposed ORing method enhances the justification of the micro cracks as clearly presented in the output image shown in Fig. 4. Evidently, the cracks are more perceptible compared to the original EL image.

The binary image determined using the proposed technique is measured using (1).

$$A = \sum_{i=0}^{n-1}\sum_{j=0}^{m-1} B[i,j] \tag{1}$$

where A is the inspected area, $B[i,j]$ is the two dimensional (2D) binary image at a position i and j, where i corresponds to horizontal axis and j is the vertical axis of the image, n and m corresponds to the vertical and horizontal iterations of the binary image processing, respectively. A greater number of n and m yields a further enhancement in the binary image, therefore, the actual cracked area would be more feasible. However, it is worth noting that a higher order of iterations lead to additional processing time required to output the binary image. As a rule of thumb, a value of 100 iterations for both variables is usually used. The position of the object in the cracked area is calculated using (2) and (3).

$$\bar{x}\ \sum_{i=0}^{n-1}\sum_{j=0}^{m-1} B[i,j] = \sum_{i=0}^{n-1}\sum_{j=0}^{m-1} j\ B[i,j] \tag{2}$$

$$\bar{y}\ \sum_{i=0}^{n-1}\sum_{j=0}^{m-1} B[i,j] = -\sum_{i=0}^{n-1}\sum_{j=0}^{m-1} i\ B[i,j] \tag{3}$$

where $\bar{x}$ and $\bar{y}$ are the coordinates of the center of the region for both healthy and examined/cracked solar cell images, respectively. The position of the cracks are determined using (4) and (5).

$$\bar{x} = \frac{\sum_{i=0}^{n-1}\sum_{j=0}^{m-1} j\ B[i,j]}{A} \tag{4}$$

$$\bar{y} = \frac{-\sum_{i=0}^{n-1}\sum_{j=0}^{m-1} i\ B[i,j]}{A} \tag{5}$$

By contrast with the results shown in Fig. 4(c), there are two pixels were compared using the OR gate function. We have reproduced the images of these pixels in Fig. 3. The output binary image is determined using equations (4) and (5). As noticed, the non-cracked image is calibrated using the while color, whereas the black area corresponds to the actual cracks affecting the examined solar cell.

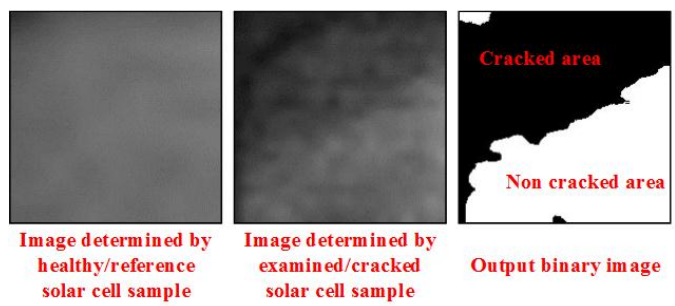

Fig. 3. Flowchart of the proposed micro crack detection technique

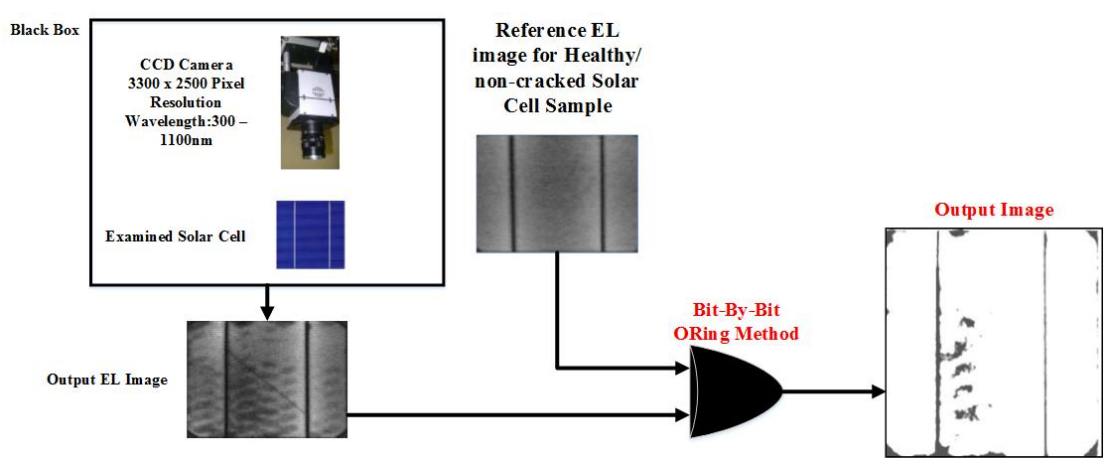

Fig. 2. Representation of the procedure to apply the ORing method

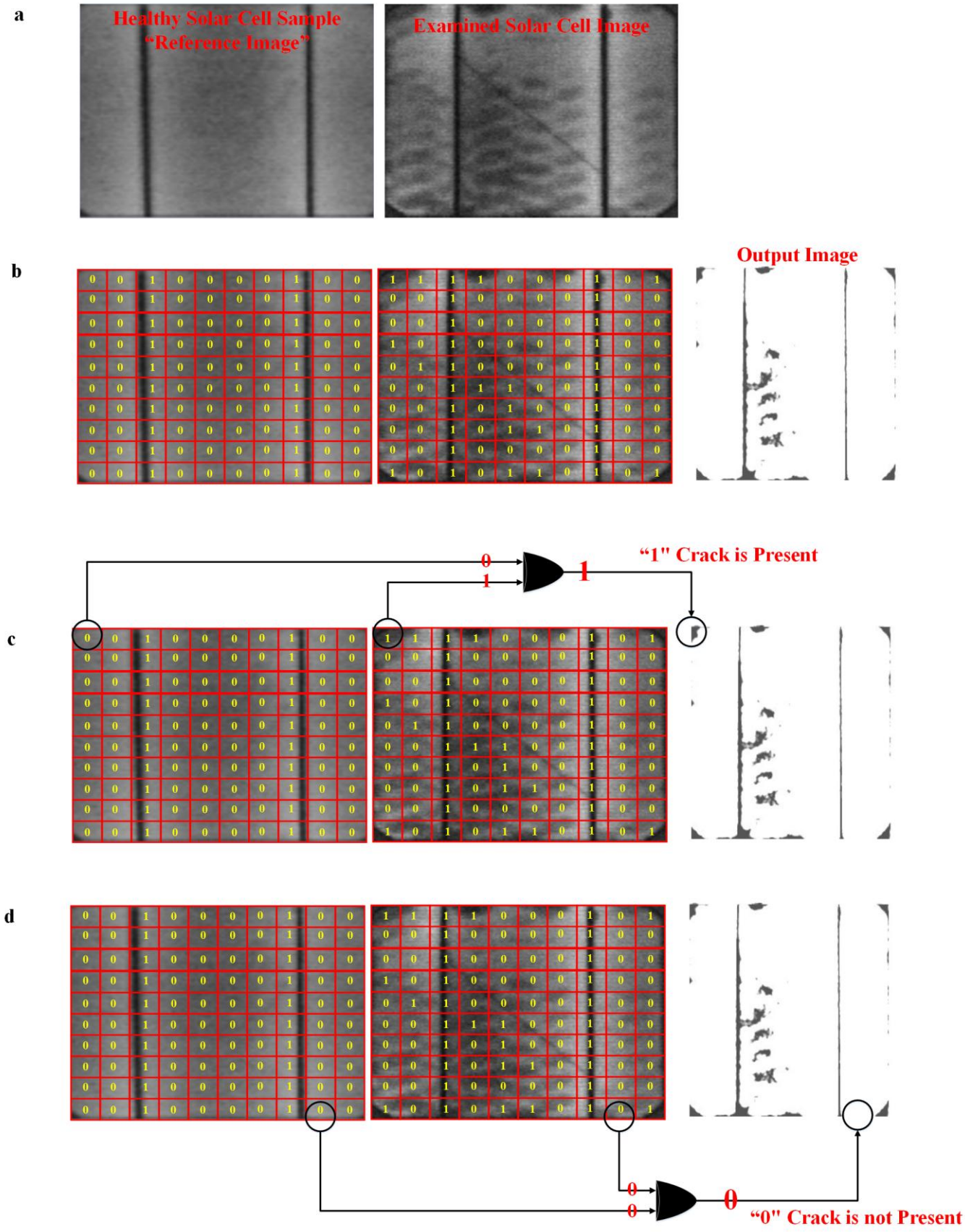

Fig. 4. (b) Healthy solar cell vs. examined solar cell samples, (b) Output image of the healthy vs. cracked solar cell image using the proposed ORing method, (c) Example for the ORing gate functionality while the result is equal to "1", (d) Example for the ORing gate functionality while the result is equal to "0"

In conclusion, the detection technique procedure is summarized in Fig. 5(a); where crack-free vs. examined solar cell output EL image has to be determined. Next, the bit-by-bit gridding for both EL images will be processed using an OR gate in order to identify whether the inspected cell is cracked. The bits of the ORing method will be processed using equations (4) and (5) in order to verity the actual size and position of the cracks. Finally, the output image will be passed into an accept/reject criterion to identify whether to accept or reject the solar cell based on the detected cracks size and position, yet the procedure of this feature for the MES will be discussed in the next section.

As the proposed technique is conditional on the detection of the EL image. Therefore, the minimum crack width or length that might be sensed is within a range of 400-700 µm [26], dependent on the resolution of the EL setup. Fig. 5(b) shows an example of a micro cracks taken at a magnification of 500 µm (0.5 mm).

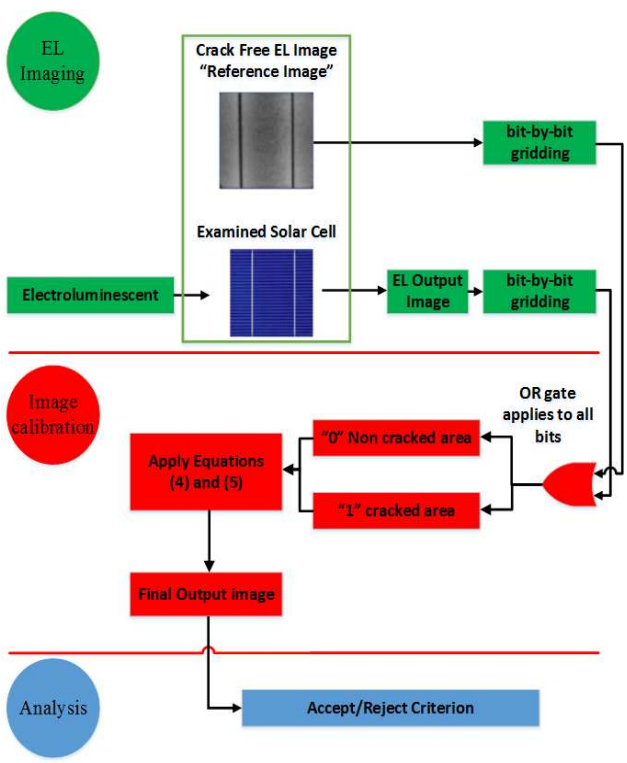

(a)

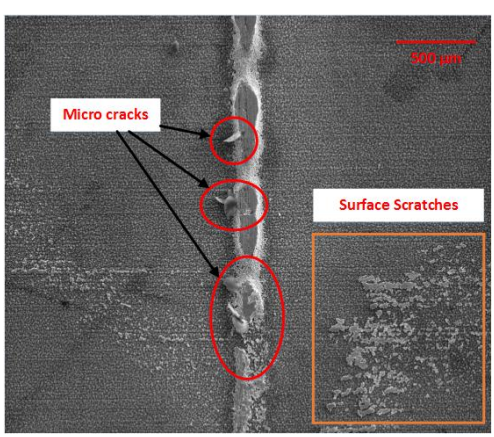

(b)

Fig. 5. (a) Flowchart of the proposed micro crack detection technique, (b) Smallest crack size that could be detected with high resolution image

IV. Solar Cell Accept/Reject Criterion

The inspected solar cell samples, after passing though the calibration mode discussed earlier in section III, the yielded image of the solar cell will be passed into a plot profile mapping. The plot profile measures the distance in pixels vs. the gray level of the image [19]; gray level corresponds to the dark areas/zones of the perceived solar cell image [20].

The main objective of the plot profile is to determine the drop in the actual gray level of the dark spots detected in the solar cell, hence, the margins of the gray level must be known by the developed inspection process. Therefore, at initial stage of development, we have determined the gray level of a healthy solar cell sample shown in Fig. 6(a), which does not contain any drack spots "cracks". The results of the experiment is shown in Fig. 6(b). As presented, the gray level is steady at a level of 254; in case the calibrated image of the EL setup contains minor adjustments, henceforth, we have modified the level of confidence for the gray level within a margin of 5%, consequently the upper and lower limits of the acceptable gray level are equal to 268 and 242, respectively. It is worth noting that as the resolution of the captured images of the EL is equal to 200 x 200 pixels, therefore, the x-axis presented on Fig. 6(a) is restricted to 200 pixels.

By contrast with the solar cell manufacturing layout, two busbars at a distance of 41-48 and 153-160 are observed. The drop in the gray level at these pixels matches the drack areas obtained by the EL image due to the existence of two busbars, yet it does not correspond to an actual crack.

At these specific intervals, the accept/reject criterion would not meditate the gray level drop as an indicator for a micro crack presence. In order to test the effectiveness of the accept/reject criterion, we have observed a cracked solar cell using the proposed method. Obtained output image of the cracks are shown in Fig. 7(a).

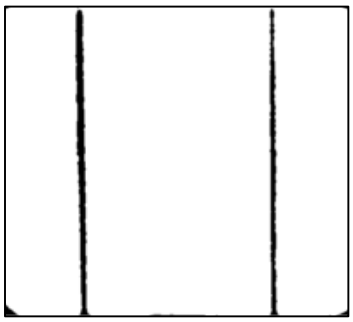

(a)

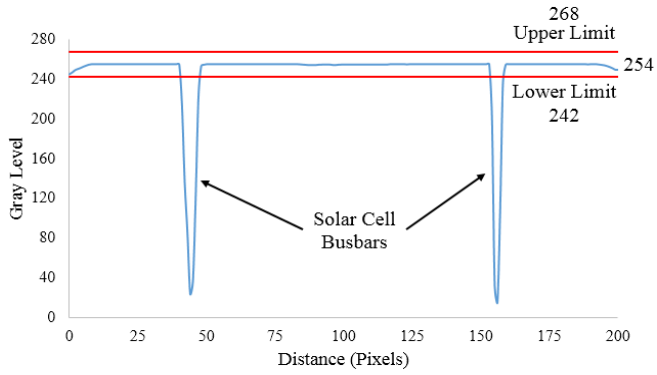

(b)

Fig. 6. (a) healthy/non-cracked solar cell output image obtained using the proposed detection method, (b) Plot profile presenting the distance vs. gray level of the solar cell sample

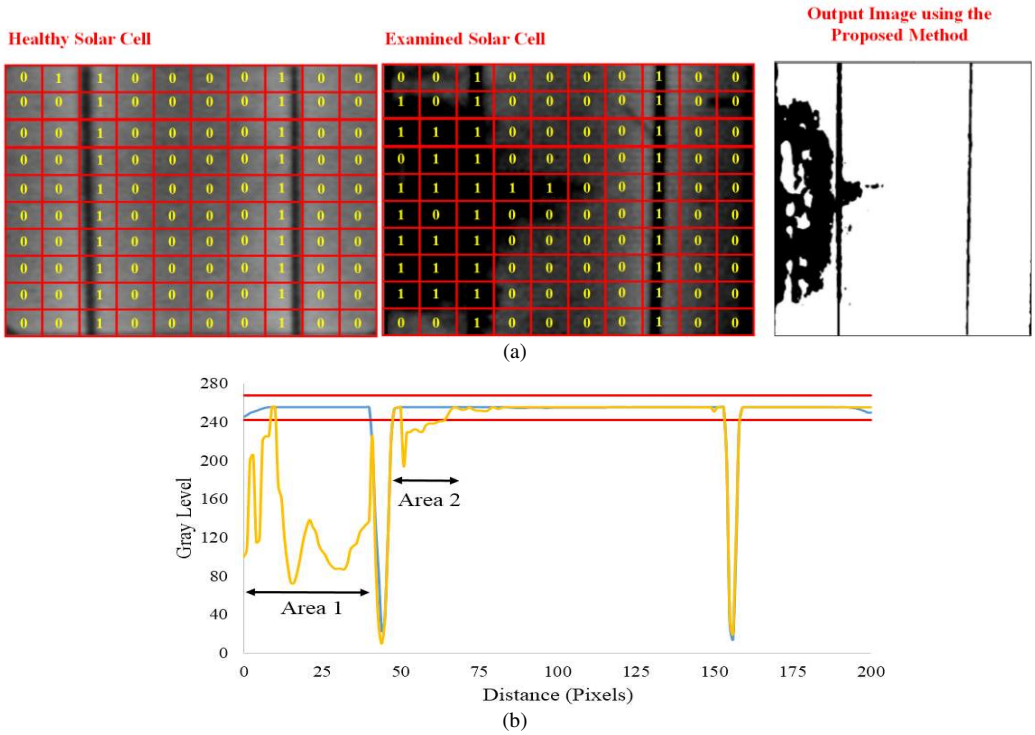

Fig. 7. (a) Cracked solar cell output image obtained using the proposed detection method, (b) Plot profile presenting the distance vs. gray level of the solar cell sample

As can be noticed, there is a major crack in the left hand-side of the examined sample. Next, as shown in Fig. 7(b), the output plot profile of the inspected sample shows that there is a drop in the gray level from 0 to 50 pixels, which corresponds to the actual cracks present in the inspected solar cell. Therefore, according to this outcome, the plot profile verifies that the sample is rejected and hence it has to be recycled and not processed into the next phase of the solar cell manufacturing executing systems.

To sum up, this section presents the development of the accept/reject criterion for the output image calibrated using the proposed micro cracks detection technique. The plot profile, using the concept of the gray level has been used to indicate whether to accept or reject the inspected solar cell sample. In the next section, a comparison between the proposed method in this article vs. several micro cracks detection techniques available in the literature will be discussed.

V. Inspection Speed

In order to evaluate the inspection speed of the proposed method, the output image of a cracked solar cell sample has been observed during several time-elapse. According to Fig. 8, the original EL image is captured within a period of 1.5 seconds; this time could typically be reduced (0.5~1 second) if the EL setup uses a field programmable gate arrays (FPGA) or any further ultra-fast processing unit. Nonetheless, in our case, the EL setup is directly connected to core i7 personal computer (PC) that would yield an increase in the acquisition time of the EL image. Interesting, the proposed detection system produces the final calibrated image of the micro cracks within a period of 1.53 seconds.

Excluding the time of the EL imaging system, the proposed ORing method would function within a period of 0.3 seconds. This is comparatively very fast acquisition of the micro cracks compared to various approaches [22-24] that would require at least several seconds to function the enhancement of the EL image.

To sum up, according to the inspection speed shown in Fig. 8, typically the proposed method is capable of enhancing the conventional EL image for at least 39 solar cell samples in one minute; this calculation includes the time where the EL image has to be captured for every inspected solar cell sample.

In the next section, the evaluation and comparison of the developed detection process will be compared against recent studies on solar cells cracks detection systems, including the technique description as well as the limitations of recent algorithms adopted to enhance the resolution of EL images.

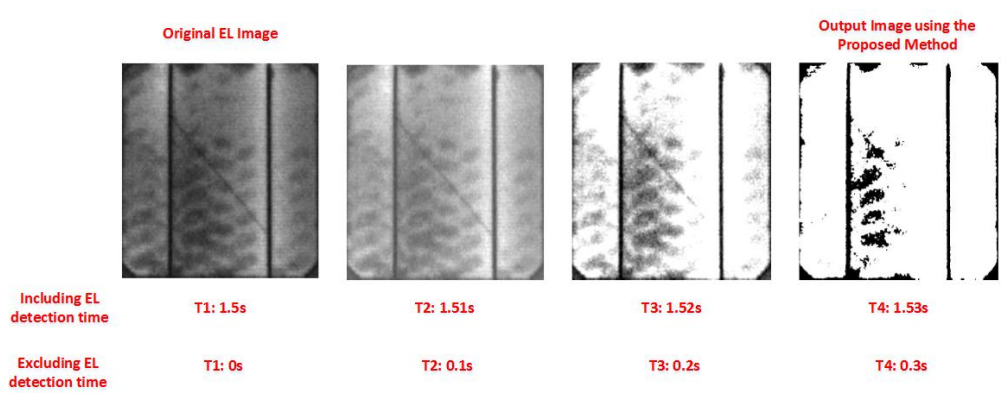

Fig. 8. Inspection speed of the proposed method

VI. Comparative Study

In order to verify the effectiveness of the proposed micro crack detection technique, the obtained results have been compared with multiple [6] and [21-24] well-developed micro cracks detection methods. A summary of the comparison is shown in Table I.

According to [6] and [23], both developed methods custom the detection of micro cracks using a Photoluminescence (PL) imaging technique. In fact, the PL signal is determined by the actual lifetime which is mostly affected by both bulk and surface recombination, and when during high spatial resolution and short measurement time, the PL imaging can be used inline during the production of silicon wafers. For example, in [6], the developed detection method enhanced the PL imaging technique using a contact less modulation for the actual obtained PL images, while a complex optical sensor and LED-based driver have to be used. Another limitation associated with this technique that it cannot identify cracks in the range of 1µm. On the other hand, in [23], the output PL image has been improved using analysis of the fill-factor and solar cell open circuit voltage. This would limit the detection area up to 90%, and it is quite complex in terms of the technique application, especially using micro cracks inline detection that is incorporated within the solar cells' manufacturing system, since main electrical parameters such as open circuit voltage and fill factor are required.

Other micro cracks detection techniques use thermal imaging such as the well-developed method proposed by W. Brooks *et al*. [21]. This method esquires can identify the noninvasive and nondestructive regions of the inspected solar cell samples. Main limitations associated with this method that is has to use a high-resolution IR camera, and there is no evidence that this technique would identify micro cracks in the range of 100µm.

Recently, multiple methods are capable of detecting micro cracks of solar cell wafers using the concept of EL imaging. In [22], an automatic defect detection scheme based on Haar-like feature extraction is developed. This method also uses a fuzzy C-means algorithms in order to enhance the layout of the detected EL image. The method is quite stable and it has a fast response in determining the output EL image. However, two automatic parameters including the distance and fuzzy clusters are needed prior to the inspection of the cracks as well as a number of crack-free and cracked solar cell samples that are required for tanning purposes.

M. Frazãoa et al. [24] developed a new approach that is capable to enhance the detection of solar cells micro cracks using EL imaging technique. The system is comprised of a light-tight black-box where housed inside is a digital Nikon D40 camera and a sample holder. The digital camera is equipped with a standard F-mount 18–55 mm lens. To allow for detection in the near infrared, the IR filter was removed and replaced with a full spectrum window of equal optical path length. The overall cost of the proposed setup is highly smaller than a scientific grade camera. As such, this type of setup should therefore enable a wider spread of use even for example in PV teaching laboratories. The main limitations associated with this method that it requires the input of two images determined using two temperature levels of 90 °C and 22 °C; this condition is not available during the manufacturing executing systems for solar cell wafers.

Table I Comparative results between the proposed method developed in this article and the one presented in [6] and [21-24]

Ref.	Year of the study	Technique			Technique Description	Limitations
		EL	PL	Thermal-Imaging		
[6]	2017	x	✓	x	An outdoor Photoluminescence (PL) imaging system is proposed using a contact less modulation technique. Used wavelength is identical with indoor EL imaging technique.	1) Optical sensors and LED driver are required to function the PL system. 2) The technique cannot detect cracks in the range of 100µm.
[21]	2015	x	x	✓	Noninvasive and nondestructive method of crack detection in crystalline Si solar cells using thermal imaging camera. The camera is detecting in the 7.5–13 µm wavelength range.	1) Expensive equipment is required such as high-resolution IR camera. 2) No evidence to detect cracks below 1µm.
[22]	2015	✓	x	x	An automatic defect detection scheme based on Haar-like feature extraction and a new clustering technique is developed. A Fuzzy C-means is used to enhance the image processing as well as the inspection of possible cracks in solar cells.	1) Multiple crack-free and cracked solar cell samples are required for tanning purposes. 2) Two parameters including the distance and fuzzy clusters are need prior to the examination of the cracks.
[23]	2016	x	✓	x	Photoluminescence (PL) imaging method is used for the quantification of defects in a-Si:H/c-Si hetero junction solar cells. The technique uses the analysis of the fill-factor and solar cell open circuit voltage for improving the detection quality.	1) Up to 90% of the total detective area is only observed. 2) The technique need further inspection of the solar cell main electrical parameters which slows the detection speed.
[24]	2017	✓	x	x	Low-cost electroluminescence (EL) technique is proposed. The Technique uses the analysis of the EL images at high and low temperature variations; empirically at 90 °C and 22 °C.	1) The speed of the detection is very slow (6 minutes), since the technique requires the images of the inspected solar cell at two different temperature levels (90 °C and 22 °C).
Proposed Method	2019	✓	x	x	A simple and reliability ORing method is used to digitally compare between the examined/cracked and a healthy/non-cracked solar cell samples. While an accept/reject criterion has also been introduced using the concept of the plot profile of the gray level for the examined solar cell samples.	1) A reference sample is required in order to run the system. 2) Mathematical calculations have to be included in the detection system to identify the position and size of the actual cracks.

By contrast with above limitations, in this article, we proposed a reliable and simple detection method that is capable of determining solar cells micro cracks using ORing method as well as the plot profile. The developed approach has only two limitations including the mathematical calculations to determine the position and size of the actual cracks of the solar cell. In addition, an EL reference image for a healthy/non-cracked solar cell sample is required for the ORing method extraction features purposes.

VII. Conclusion

A novel solar cell micro crack detection system for use in manufacturing execution system has been developed and presented. The proposed technique uses an ORing method that is capable of digitally enhance the output images of the conventional EL imaging technique. This relies on the mechanism where the examined solar cell EL image is compared with a reference healthy solar cell EL image using the ORing bit-by-bit method. The output image is then processed using a plot profile which is acknowledged as the distance in pixels against the gray level, this step would identify whether the detected micro cracks are within acceptable level or the inspected solar cell wafer has to be rejected and recycled. The crack detection system has been shown to be beneficial with the rapid real-time data acquisition necessitated by cell layout and tabbing phases in the PV wafer manufacturing process.

References

[1] S. Ostapenko. U.S. Patent No. 9,933,394. Washington, DC: U.S. Patent and Trademark Office, 2018.

[2] M. Dhimish, P. Mather and V. Holmes, "Evaluating Power Loss and Performance Ratio of Hot-Spotted Photovoltaic Modules," in IEEE Transactions on Electron Devices, vol. 65, no. 12, pp. 5419-5427, Dec. 2018, doi: 10.1109/TED.2018.2877806.

[3] R. Yang et al., "Electromagnetic Induction Heating and Image Fusion of Silicon Photovoltaic Cell Electro-Thermography and Electroluminescence," in IEEE Transactions on Industrial Informatics, doi: 10.1109/TII.2019.2922680.

[4] Y. Wu, X. Yang, W. Chen, Y. Yue, M. Cai, F. Xie, E. Bi, A. Islam and L. Han, "Perovskite solar cells with 18.21% efficiency and area over 1 cm2 fabricated by heterojunction engineering," in Nature Energy, vol. 1, no. 11, pp. 16148, Sep. 2016, doi: 10.1038/nenergy.2016.148.

[5] Y. Zhu, M. K. Juhl, T. Trupke and Z. Hameiri, "Photoluminescence Imaging of Silicon Wafers and Solar Cells With Spatially Inhomogeneous Illumination," in IEEE Journal of Photovoltaics, vol. 7, no. 4, pp. 1087-1091, July 2017, doi: 10.1109/JPHOTOV.2017.2690875.

[6] R. Bhoopathy, O. Kunz, M. Juhl, T. Trupke and Z. Hameiri, Z, "Outdoor photoluminescence imaging of photovoltaic modules with sunlight excitation," in Progress in Photovoltaics: Research and Applications, vol. 26, no. 1, pp. 69-73, Sep. 2017, doi: 10.1002/pip.2946.

[7] M. Dhimish et al., "The impact of cracks on the performance of photovoltaic modules," 2017 IEEE Manchester PowerTech, Manchester, 2017, pp. 1-6, doi: 10.1109/PTC.2017.7980824.

[8] A. M. Hilton, A. D. Cahill and E. R. Heller, "A Comparison of Electroluminescence Spectra From Plan View and Cross-Sectioned AlGaN/GaN Devices," in IEEE Transactions on Electron Devices, vol. 65, no. 1, pp. 59-63, Jan. 2018, doi: 10.1109/TED.2017.2775101.

[9] R. Schurch, S. M. Rowland, R. S. Bradley and P. J. Withers, "Comparison and combination of imaging techniques for three dimensional analysis of electrical trees," in IEEE Transactions on Dielectrics and Electrical Insulation, vol. 22, no. 2, pp. 709-719, April 2015, doi: 10.1109/TDEI.2014.004730.

[10] M. Dhimish and P. Mather, "Development of Novel Solar Cell Micro Crack Detection Technique," in IEEE Transactions on Semiconductor Manufacturing, vol. 32, no. 3, pp. 277-285, Aug. 2019, doi: 10.1109/TSM.2019.2921951.

[11] J. Käsewieter, F. Haase and M. Köntges, "Model of Cracked Solar Cell Metallization Leading to Permanent Module Power Loss," in IEEE Journal of Photovoltaics, vol. 6, no. 1, pp. 28-33, Jan. 2016, doi: 10.1109/JPHOTOV.2015.2487829.

[12] Z. Liu, M. Peters, V. Shanmugam, Y. K. Khoo, S. Guo, R. Stangl, A. G. Aberle and J. Wong, "Luminescence imaging analysis of light harvesting from inactive areas in crystalline silicon PV modules," in Solar Energy Materials and Solar Cells, vol. 144, pp. 523-531, Jan. 2016, doi: 10.1016/j.solmat.2015.09.013.

[13] S. Oh et al., "Control of Crack Formation for the Fabrication of Crack-Free and Self-Isolated High-Efficiency Gallium Arsenide Photovoltaic Cells on Silicon Substrate," in IEEE Journal of Photovoltaics, vol. 6, no. 4, pp. 1031-1035, July 2016, doi: 10.1109/JPHOTOV.2016.2566887.

[14] Y. He, B. Du and S. Huang, "Noncontact Electromagnetic Induction Excited Infrared Thermography for Photovoltaic Cells and Modules Inspection," in IEEE Transactions on Industrial Informatics, vol. 14, no. 12, pp. 5585-5593, Dec. 2018, doi: 10.1109/TII.2018.2822272.

[15] M. Abdelhamid, R. Singh and M. Omar, "Review of Microcrack Detection Techniques for Silicon Solar Cells," in IEEE Journal of Photovoltaics, vol. 4, no. 1, pp. 514-524, Jan. 2014, doi: 10.1109/JPHOTOV.2013.2285622.

[16] B. Du, R. Yang, Y. He, F. Wang and S. Huang, "Nondestructive inspection, testing and evaluation for Si-based, thin film and multi-junction solar cells: An overview," in Renewable and Sustainable Energy Reviews, vol. 78, pp. 1117-1151, Oct. 2017, doi: 10.1016/j.rser.2017.05.017.

[17] M. Dhimish, V. Holmes, B. Mehrdadi and M. Dales, "The impact of cracks on photovoltaic power performance," in Journal of Science: Advanced Materials and Devices, vol. 2, no. 2, pp. 199-209, June 2017, doi: 10.1016/j.jsamd.2017.05.005.

[18] M. Bliss, X. Wu, K. G. Bedrich, J. W. Bowers, T. R. Betts and R. Gottschalg, "Spatially and spectrally resolved electroluminescence measurement system for photovoltaic characterisation," in IET Renewable Power Generation, vol. 9, no. 5, pp. 446-452, 7 2015, doi: 10.1049/iet-rpg.2014.0366.

[19] M. Dhimish, V. Holmes and P. Mather, "Novel Photovoltaic Micro Crack Detection Technique," in IEEE Transactions on Device and Materials Reliability, vol. 19, no. 2, pp. 304-312, June 2019, doi: 10.1109/TDMR.2019.2907019.

[20] M. Dhimish, V. Holmes, P. Mather, C. Aissa and M. Sibley, "Development of 3D graph-based model to examine photovoltaic micro cracks," in Journal of Science: Advanced Materials and Devices, vol. 3, no. 3, pp. 380-388, Sep. 2018, doi: 10.1016/j.jsamd.2018.07.004.

[21] W. S. M. Brooks, D. A. Lamb and S. J. C. Irvine, "IR Reflectance Imaging for Crystalline Si Solar Cell Crack Detection," in IEEE Journal of Photovoltaics, vol. 5, no. 5, pp. 1271-1275, Sept. 2015, doi: 10.1109/JPHOTOV.2015.2438636.

[22] D. Tsai, G. Li, W. Li and W. Chiu, "Defect detection in multi-crystal solar cells using clustering with uniformity measures," in Advanced Engineering Informatics, vol. 29, no. 3, pp. 419-430, Aug. 2015, doi: 10.1016/j.aei.2015.01.014.

[23] O. Nos, W. Favre, F. Jay, F. Ozanne, A. Valla, J. Alvarez, D. Muñoz and P. J. Ribeyron, "Quality control method based on photoluminescence imaging for the performance prediction of c-Si/a-Si:H heterojunction solar cells in industrial production lines," in Solar Energy Material and Solar Cells, vol. 144, pp. 210-220, Jan. 2016, doi: 10.1016/j.solmat.2015.09.009.

[24] M. Frazãoa, J. A. Silvab, K. Lobatob and J. M. Serrab, "Electroluminescence of silicon solar cells using a consumer grade digital camera," in Measurement, vol. 99, pp. 7-12, March 2017, doi: 10.1016/j.measurement.2016.12.017.

[25] Sensovation. (2019). SensoCam Cameras from Sensovation - De-signed for Electroluminescence Inspection . Retrieved from https://www.sensovation.com/com/Applications/Photovoltaic.

[26] M. Dhimish, "Micro cracks distribution and power degradation of polycrystalline solar cells wafer: Observations constructed from the analysis of 4000 samples," in Renewable Energy, vol. 145, pp. 466-477, Jan. 2020, doi: 10.1016/j.renene.2019.06.057.

Appendix A

CCD camera specifications [25]:

- Customized grade Si-CCD sensors
- Excellent near IR sensitivity (1000 to 1100 nm)
- Spatial Resolution up to 63µm on 156mm x 156mm cell sample
- 4-stage TE cooling of CCD for ultra-low noise imaging
- 16 bit dynamic range
- Imaging speed of 1 image/seconds